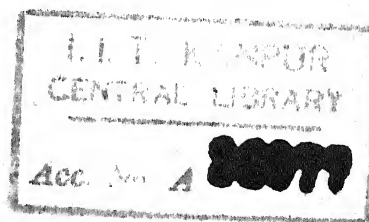


A MEDIUM RESOLUTION MASS SPECTROMETER FOR GAS - VAPOUR ANALYSIS

A Thesis Submitted
In Partial Fulfilment of the Requirements
for the Degree of
MASTER OF TECHNOLOGY

By
R. NAGARAJAN

Thesis
543.07
N 131



A 26077

✓
CHE-1973-M-NAG-MED

to the

DEPARTMENT OF CHEMICAL ENGINEERING
INDIAN INSTITUTE OF TECHNOLOGY KANPUR
MAY 1973

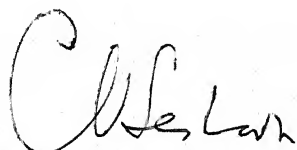
(ii)

CERTIFICATE

This is to certify that this work has been carried out under our supervision and has not been submitted elsewhere for a degree.

Dated May 4, 1973

Dr. P.K. Ghosh
Assistant Professor
Department of Chemistry
Indian Institute of Technology
Kanpur-208016, India


Dr. C.V. Seshadri
Associate Professor
Department of Chemical Engg.
Indian Institute of Technology
Kanpur-208016, India

POST GRADUATE OFFICE
This thesis has been approved
for the award of Degree of
Master of Technology (M.Tech.)
in accordance with the
regulations of the Indian
Institute of Technology Kanpur
Dated. 24.8.73 24

ACKNOWLEDGEMENTS

While fifteen pages are sufficient to contain this thesis, the acknowledgements of the assistance I received would run to innumerable pages. Only those involved could recognise how such collective participation is necessary for achieving any progress in the work undertaken. Without this collective effort nothing would have been achieved. While many are bound to go unacknowledged, I should mention the following few:

Dr. C.V. Seshadri (Chemical Engineering) - First for taking "care" of me - whether it is hostel accommodation or financial troubles or ... Secondly, but most importantly for his continuous encouragement in all my work which has always been a source for enthusiasm.

Dr.P.K. Ghosh (Chemistry) - Fourteen hours per day of work- he has been a part of it along with me for ~~many~~ day. To say the least, all that I have learnt in this institute has been in his laboratory.

I acknowledge among others the assistance of -

Dr. G.K. Mehta (Physics) and Dr. V. Subba Rao (Chemical Engineering)- for unhesitatingly providing me with materials and instruments whenever I needed.

Dr. Martin C. Berdahl (Jet Propulsion Laboratory deputed to Central Instrumentation Service) - for the design and fabrication of the electronic circuitry and troubleshooting at a moments' call from me.

Staff of Central Instrumentation Service - for the help in loaning and repairing power supplies, recorders etc.

V.L. Rajani, S.L. Yadav, V.L. Yadav, A. Mazumdar (Central Workshop) - for a variety machining jobs including quadrupole mounts, quadrupole rods, vacuum connections, ion sources etc.

Dr. Prithipal Singh (Metallurgy) - for the soldering and welding jobs including the silver soldering of the ceramic pieces to stainless steel quadrupole rods.

Jasbir Singh (my labmate for an year) - For the design and fabrication of the rf amplifier.

Amit Hui, Hegde, Utpal Roychaudhry (my labmates for the last

(iv)

three years) - no work would have been accomplished without them.

S.P. Rajagopalan, K.C. Rao (my fellow students) - for running to computer centre on my behalf.

D.S. Panesar (Chemical Engineering) - for the drawings

B.S. Pandey (Chemical Engineering) - for the typing

I MUST SAY THAT THIS IS NOT MY WORK BUT THEIR WORK.

CONTENTS

			Page
	List of Figures	...	(vi)
	List of Symbols	...	(vii)
	Abstract	...	(viii)
1.	INTRODUCTION	...	1
1.1	Mass Spectrometers for Chemical Process Control	...	
1.2	Basic Operation of Quadrupole Mass Spectrometer	...	
1.3	Advantages of the Quadrupole Mass Spectrometer	...	
1.4	Objectives of This Work	...	
2.	THEORY OF OPERATION OF QUADRUPOLE MASS SPECTROMETER	...	6
2.1	Electrode Structure and Quadrupole Field		
2.2	Equations of Ion Motion	...	
2.3	Solutions to the Equations of Motion		
2.4	Stability Diagram	...	
2.5.	Ion Trajectories in the Quadrupole Field		
3.	EFFECT OF INITIAL CONDITIONS ON ION TRANSMISSION	...	14
3.1	Maximum Amplitude of Ion Motion	...	
3.2	Results of Computation	...	
3.3	Conclusions from Present Computations		
4.	QUADRUPOLE MASS SPECTROMETER DESIGN		23
4.1	Mechanical Design	...	
4.2	Electronic Design	...	
5.	EXPERIMENTS, RESULTS AND CONCLUSIONS		31
	REFERENCES	...	34

LIST OF FIGURES

FIGURE		PAGE
1	Schematic of Quadrupole Mass Spectrometer	3
2	Schematic of Field Configuration	7
3	Stability Diagram for both X and Y.	7
4	Ion Trajectory in X-Z Plane ...	12
5	Ion Trajectory in Y-Z Plane ...	12
6	Maximum Amplitudes at Different Resolutions	15
7	Effect of Initial Radial Velocity at 200 Resolution ...	17
8	Effect of Initial Radial Velocity at 500 Resolution ...	18
9	Effect of Initial Displacement at 70 Resolution ...	19
10	Effect of Initial Phase at Different β Values ...	20
11	100% Ion Transmission Contours ...	21
12	Schematic of Ion Source ...	24
13	Schematic of Quadrupole Mounting	24
14	Quadrupole Power Supply - Crystal Oscillator with tube Amplifier ...	26
15	AC/DC Excitation Matching Network	27
16	Transistorised rf Amplifier ...	28
17	Typical Mass Spectrum ...	32

LIST OF SYMBOLS

ϕ	Potential at any point in the field
ϕ_0	Potential at the electrode surface
r_0	Quadrupole field radius
U	Quadrupole d.c. potential
V	Quadrupole rf potential
ω	Quadrupole rf frequency
E	Electric field
e	Electronic charge
m	Mass of the ion
X_M, Y_M	Maximum amplitude of ion motion in X and Y directions
$\frac{m}{\Delta m}$	Resolution of the mass spectrometer given by
$\frac{m}{\Delta m} = \frac{0.357}{0.23699 - a_{0.706}}$	
$a_{0.706}$ value of non-dimensional number a at $q = 0.706$ in the mass scan line	

1. INTRODUCTION

1.1. Mass Spectrometers for Chemical Process Control:

Process control in the chemical industries is effected through various methods. But most of them are confined to the control of process parameters like flow rates, levels, temperature, pressure etc. While it is necessary to keep these process variables controlled, it is imperative that methods of control through product analysis should be evolved as the final product quality is of greatest concern to us. This implies that procedures of analysis of final products should be evolved and the results of this analysis should be transformable into controlling signals. Some methods of analysis have come into vogue in the past such as refractometry, colorimetry, absorption spectrometry, polarography, gas chromatography etc. All these methods are based on the physical properties of the sample such as mechanical properties, electrical properties, thermal properties etc. The use of these methods remain limited due to this dependence.

A recent entry into this field has been made by mass spectrometers which do not have this disadvantage of the other analytical instruments. Mass spectrometers determine directly the mass number of the sample species. Currently a combination of gas chromatographs with mass spectrometers is widely used for chemical analysis. Of the great variety of mass spectrometers available, Quadrupole mass spectrometers offer some advantage over others because of their character-

istics. Since these are also less expensive Quadrupole mass spectrometers have the potential of in situ process control in chemical industries.

1.2 Basic operation of Quadrupole Mass Spectrometer:

Unlike most other mass spectrometers, the quadrupole mass spectrometer does not require a magnetic field. A typical quadrupole mass spectrometer is shown in Fig. 1. The principal elements constituting the mass spectrometer are the ion source, the quadrupole mass analyser and the ion collector (or detector). The whole system operates under high vacuum.

The gas to be analyzed is ionised by bombardment by an electron beam which is usually from a hot filament. As a result of this electron bombardment a small percentage of the gas atoms or molecules gets ionized. These ions are accelerated and through an entrance aperture enter the radio-frequency electric field in the mass analyser region. The field conditions (to be discussed later) cause a filtering action on the ion beam. This filtering results from the mass analyser permitting only those ions of a specific range of mass to charge ratio to completely pass the field length. These ions have bounded trajectories and they pass through to the exit aperture. All other ions have unbounded trajectories and are collected on the rods constituting the quadrupole.

The ions that travel through the analyser are ultimately collected on the ion collector. The output current

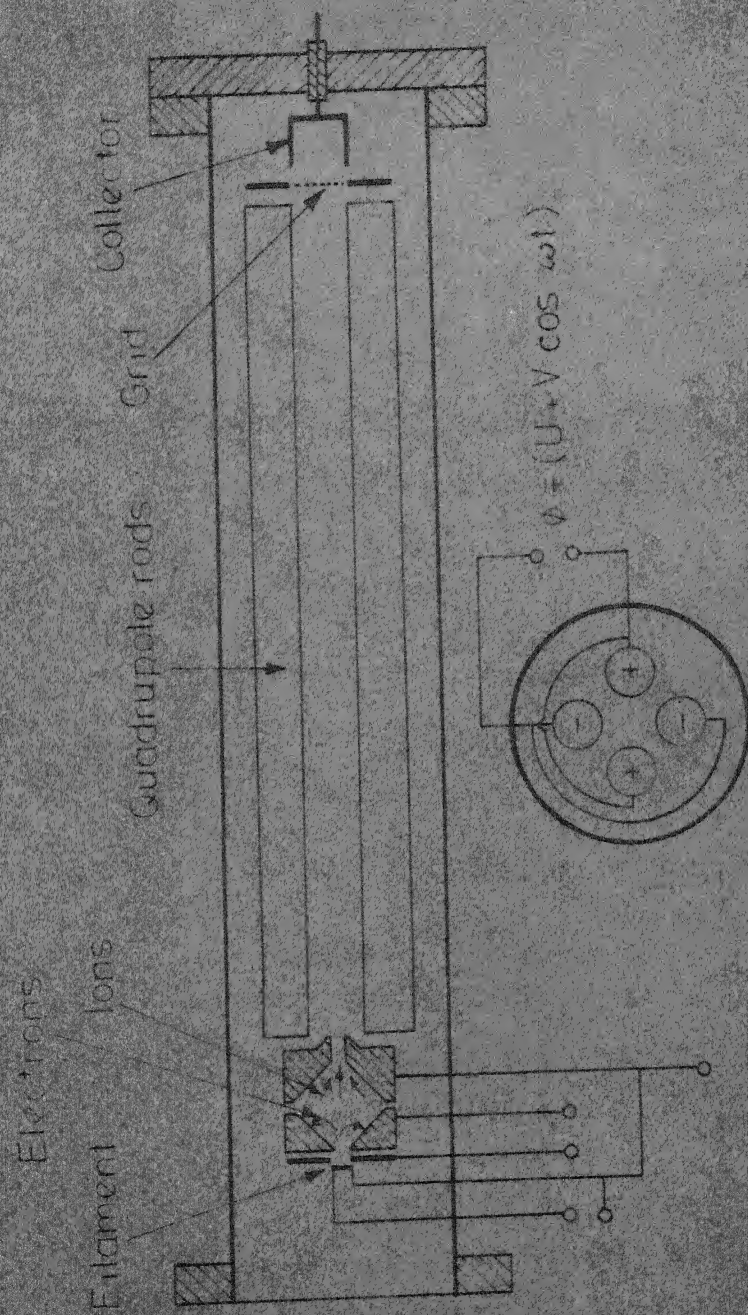


Fig. 1—Schematic of Quadrupole Mass Spectrometer

from the collector is proportional to the amount of the particular species in the given sample, assuming idealized conditions in the ion source. The charge to mass ratio satisfying the criterion for a bounded trajectory and passage through the field length is linearly related to the potentials on the quadrupole rods. Thus calibration with any known pure gas sample is sufficient to identify any other component.

1.3 Advantages of the Quadrupole Mass Spectrometer:

Since the quadrupole mass spectrometer is non-magnetic, the instrument is light in weight and problems of magnetic screening where stray magnetic fields might interfere with the system under observation are avoided. Since the principle of mass separation in the quadrupole mass analyser is unaffected by the collisions between the particles, the instrument can be used at relatively high pressure. The mass analyser's relative insensitivity to the initial velocity of ions along the analyser axis enables its use where there is a spread in the initial ion energy. The linear relation between the charge to mass ratio and the quadrupole electric potential, makes it simpler to use. The mass spectrometer is simple in its configuration and compact in design. These features of this mass spectrometer permit its wide use in various fields.

1.4. Objectives of this Work:

✓ In this work the permissible entry conditions of ions

have been computed. These data aid in designing the ion source and entry aperture of the mass analyser. A medium resolution mass spectrometer has been fabricated and has been used as a residual gas analyser. ✓

2. THEORY OF OPERATION OF QUADRUPOLE MASS SPECTROMETER

2.1. Electrode Structure and Quadrupole Field:

The quadrupole electric field is such that it is linearly related to the distance of the ion from the axis. This type of field has the nature of focusing the ions at the axis. This field is produced by a potential of the form

$$\phi = \phi_0 (ax^2 + by^2 + cz^2) \quad \dots \quad (1)$$

where a, b, c are constants characteristic of the particular field. If there is no space charge within the electrode structure, the potential must satisfy Laplace's equation

$$\nabla^2 \phi = 0. \text{ This yields}$$

$$a + b + c = 0 \quad \dots \quad (2)$$

If the field is two-dimensional and taking z to be the axis of symmetry, we get

$$c = 0; \quad a = -b = 1/r_0^2 \text{ (say)} \quad \dots \quad (3)$$

$$\phi = \phi_0 \left(\frac{x^2 - y^2}{r_0^2} \right) \quad \dots \quad (4)$$

This potential can be produced by a configuration as in Fig. 2. of four hyperbolic surfaces located so as to correspond to equipotential lines of the quadrupole field. The voltage $\phi_0 = (U + V \cos \omega t)$ is applied to the electrodes with the centre of the field chosen as the zero of the potential. The potential at any point is then

$$\phi = (U + V \cos \omega t) \left(\frac{x^2 - y^2}{r_0^2} \right) \quad \dots \quad (5)$$

The x direction is that through the centres of the pair of

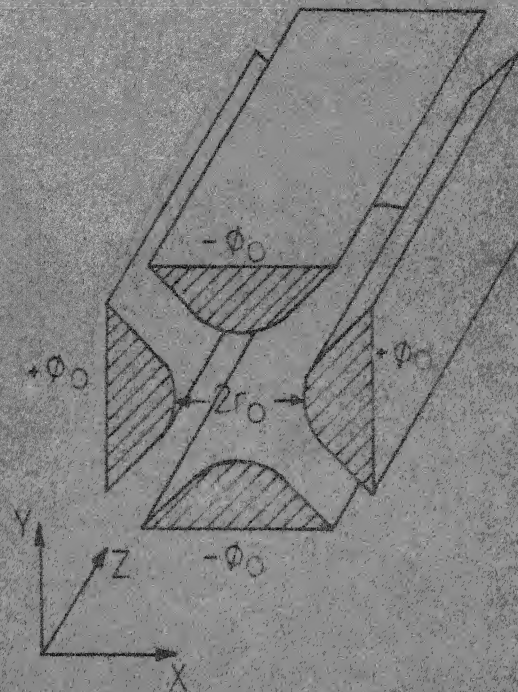


Fig. 2 - Schematic of field configuration

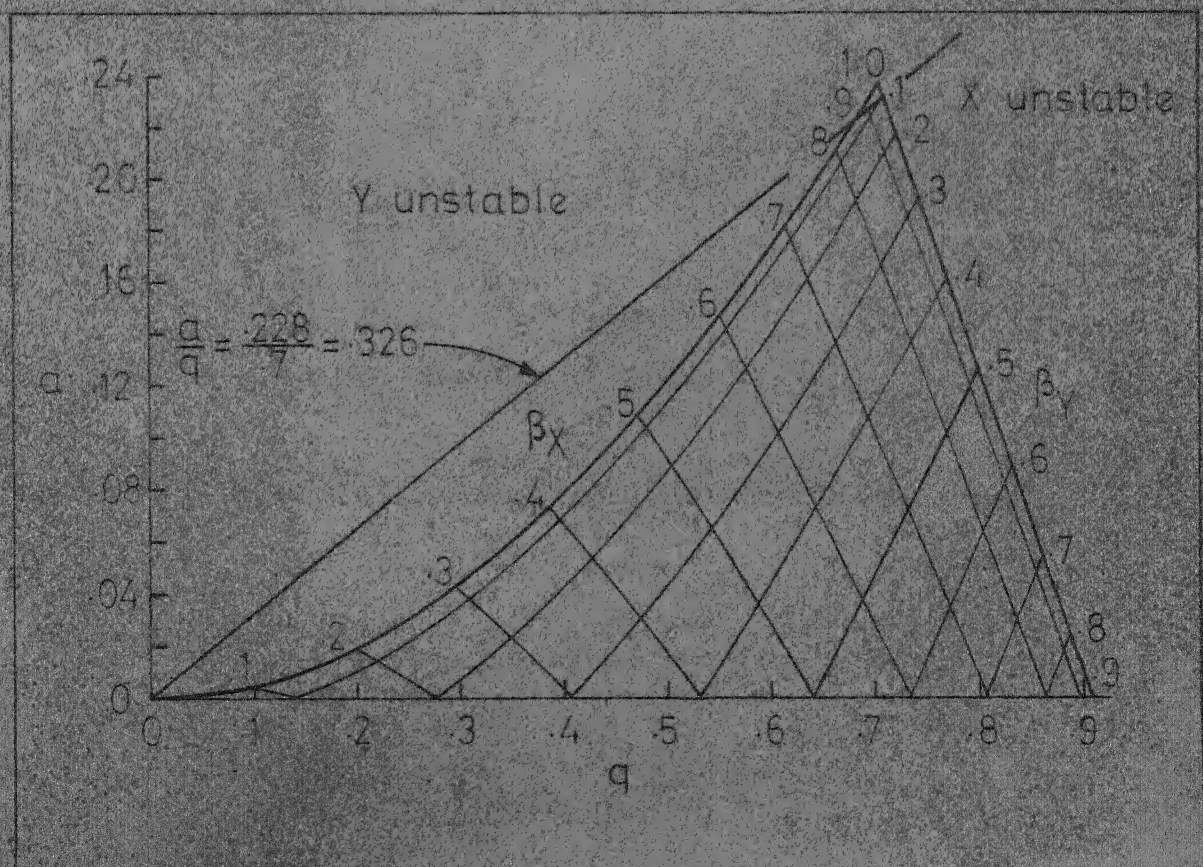


Fig. 3 - Stability diagram for both X and Y

rods for which the dc component is positive with respect to the second pair.

2.2 Equations of Ion Motion:

The electric fields obtained from the quadrupole potential (Eq.5) are

$$\begin{aligned} E_x &= - \frac{\partial \phi}{\partial x} = - (U + V \cos \omega t) \frac{2x}{r_0^2} \\ E_y &= - \frac{\partial \phi}{\partial y} = + (U + V \cos \omega t) \frac{2y}{r_0^2} \quad \dots \quad (6) \\ E_z &= - \frac{\partial \phi}{\partial z} = 0 \end{aligned}$$

The equations of motion of a singly charged ion of mass m are

$$\begin{aligned} \frac{d^2 x}{dt^2} + \frac{e}{m} (U + V \cos \omega t) \frac{2x}{r_0^2} &= 0 \\ \frac{d^2 y}{dt^2} - \frac{e}{m} (U + V \cos \omega t) \frac{2y}{r_0^2} &= 0 \quad \dots \quad (7) \\ \frac{d^2 z}{dt^2} &= 0 \end{aligned}$$

The motion in each coordinate direction is thus independent of the motion in the other directions. Introducing the substitutions

$$\begin{aligned} \omega t &= 2\xi \\ a &= 8eU/mr_0^2 \omega^2 \\ q &= 4eV/mr_0^2 \omega^2 \end{aligned} \quad \dots \quad (8)$$

(Eq.7) can be reduced to

$$\begin{aligned} \frac{d^2 x}{d\xi^2} + (a + 2q \cos 2\xi) x &= 0 \\ \frac{d^2 y}{d\xi^2} - (a + 2q \cos 2\xi) y &= 0 \quad (9) \\ \frac{d^2 z}{d\xi^2} &= 0 \end{aligned}$$

These differential equations are of the type known as Mathieu's

equations. The properties of the Mathieu equations are well known(1). We are primarily interested in the solutions that result in stable or bounded ion motion.

2.3 Solutions to the Equations of Motion:

Solutions to the Mathieu equation can be expressed in the form

$$u = \alpha' e^{\mu \xi} \sum_{-\infty}^{+\infty} c_{2s} e^{2is\xi} + \alpha'' e^{-\mu \xi} \sum_{-\infty}^{+\infty} c_{2s} e^{-2is\xi} \quad (10)$$

where u is x or y . The solutions are of two types, solutions denoted "stable" where u remains finite as $\xi \rightarrow \infty$ and "unstable" where u increases without limit as $\xi \rightarrow \infty$. The constant μ determines the type of solution. μ depends upon the values of a and q , and is independent of the initial conditions. If μ is real and non-zero, instability will arise from either the $e^{\mu \xi}$ or $e^{-\mu \xi}$ factor. There are three other possibilities:

1. $\mu = i\beta$ is purely imaginary and β is not a whole number. The solutions are stable.
2. μ is a complex number. The solutions are unstable (assuming that u_0 and u'_0 are not both zero)
3. $\mu = in$ is purely imaginary and n is an integer. The solutions are periodic but unstable.

Since μ depends on a and q , the regions of stable operation can be plotted in a - q space. Such a figure is known as the stability diagram. The stable areas with large a, q values correspond to ion motion in which the amplitudes of

oscillation are too large to be useful in practical devices. The stability area near the origin is of practical significance. The stability limits are $\beta = 0$ and $\beta = 1$.

2.4 Stability Diagram:

For an ion to traverse the mass filter, it must have stable trajectories in both x and y directions. We can superimpose the stability diagrams for x and y directions to determine the stability region for the mass filter as shown in Fig.3. A line on the stability diagram with slope a/q called mass scan line is defined if the ratio of dc to rf voltage is fixed since a/q equals $2U/V$. The apex of the stability triangle lies at $q_{\text{limit}} = 0.70600$ and $a_{\text{limit}} = 0.23699$. Consider a mass scan line as shown in Fig. 3. For any chosen values of U and hence V, ions of differing e/m will be spread out along the line according to their (a, q) values, with ions of larger e/m farthest from the origin. This mass spread can be reduced by increasing the ratio a/q i.e. U/V . This spread can be made as narrow as desired to permit only one mass to pass through the field. All the other ions will execute unstable oscillations, strike the electrodes and will be removed. This is the fundamental filtering action of the quadrupole field.

The mass scanning can be done by varying any of the field conditions ω , U or V since practically r_0 cannot be varied. Maintaining tuned circuits in the amplifier stages over a frequency range is the most serious drawback of the

variable frequency method. Since a and q vary as $\frac{1}{\omega^2}$ the frequency would also have to change as the square root of the control function if the mass peaks are to appear in a linear fashion. Hence varying ω is generally not recommended. Keeping either one of them constant, U or V can be changed to obtain the mass spectrum. But this results in shifting the scan line during the scanning thus introducing a continuous variation in resolution. Hence this method is also not recommended. By varying the magnitude of U or V keeping constant the ratio U/V and ω , each ionic species may be brought in turn into the area for stability in both x and y directions and can be transmitted through the device. Ions with e/m greater than the stable species have unstable trajectories in the x direction and ions with e/m lower than stable ions are unstable in y direction.

2.5 Ion Trajectories in the Quadrupole Field:

Typical ion trajectories in the xz and yz planes are illustrated in Fig.4 and Fig.5 respectively. The stability criterion of ions in the field does not depend on the initial conditions of ions at the entrance aperture such as the initial velocity (radial or axial), initial position and entrance phase angle. However this independence is somewhat hypothetical since the stability criterion considers only the conditions that the ions be either bounded or unbounded. The initial conditions have an effect on the practical stability since the field

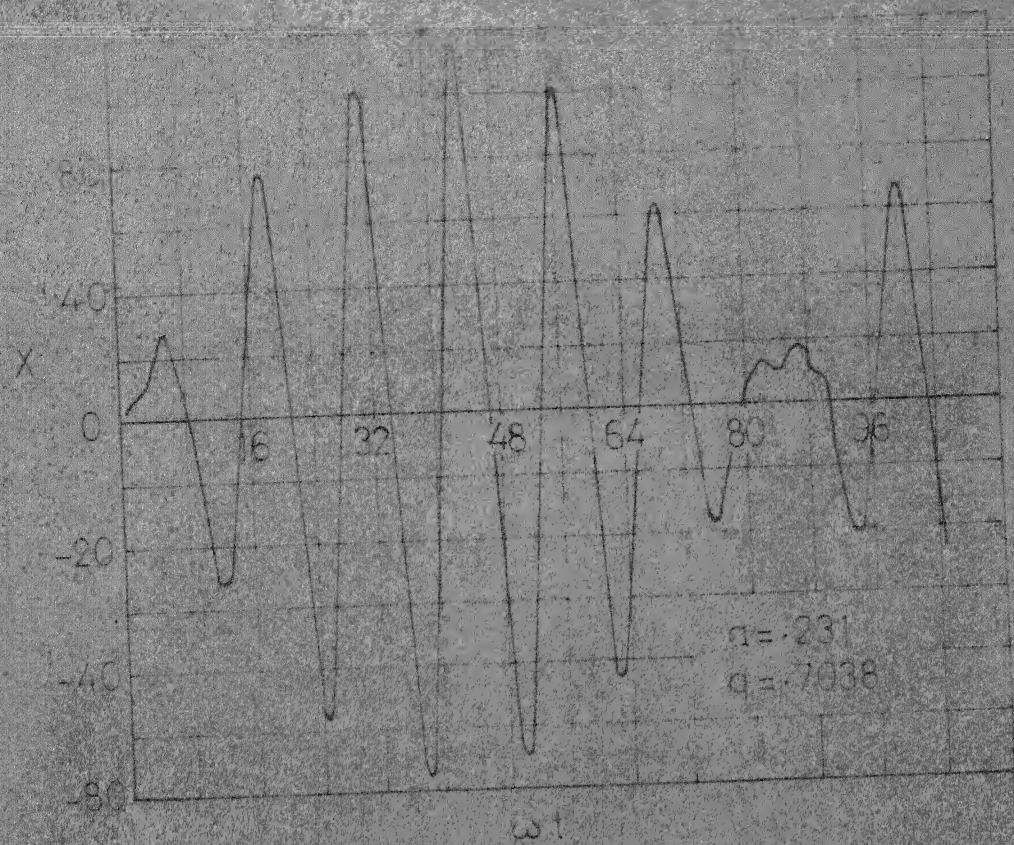


Fig 4 - Ion trajectory in X-Z plane.

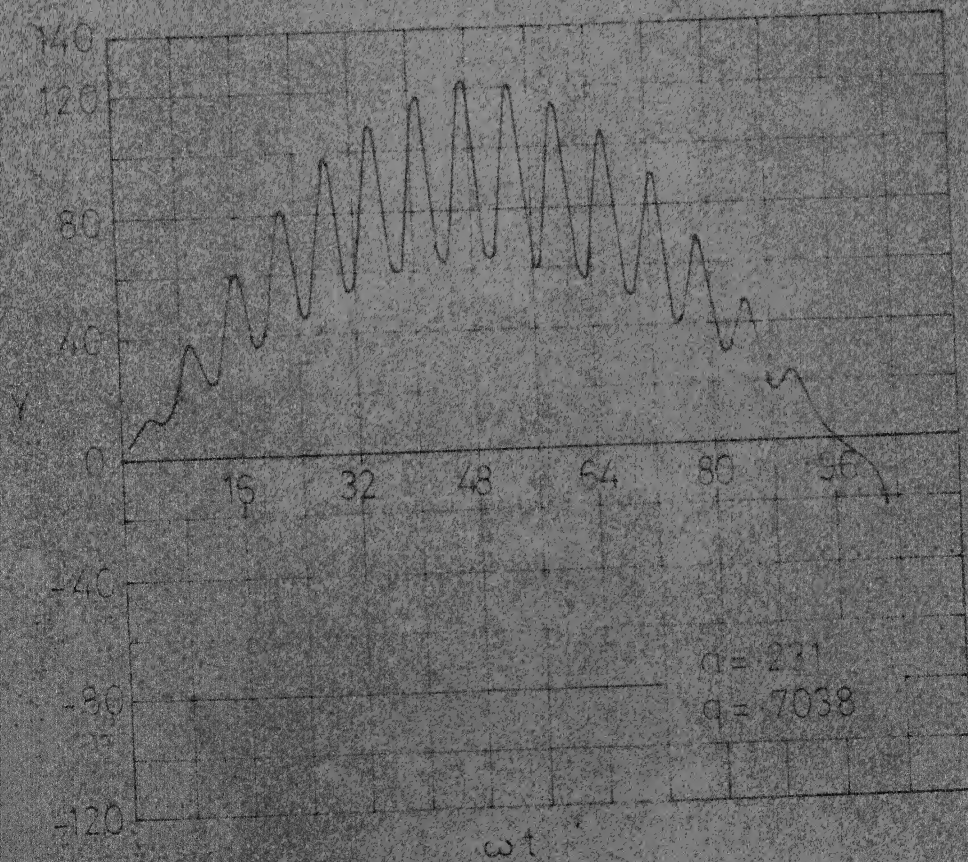


Fig 5 - Ion trajectory in the Y-Z plane.

i.e. field diameter and field length are finite.

If the radial velocity of ions at entry exceeds a limiting value, then even though the ions may have bounded oscillations, they would strike the electrode and be removed. Hence there would be a reduction in the expected value of transmission of ions. If the radial velocity of the ions at entry is below a limiting value, then even though the ion oscillations may be unstable it would pass through the finite field length without striking the electrodes. Hence there would be a reduction in the expected value of resolution. Similar limits are imposed by the initial position of ions also. Hence of practical importance here, is the placing of limits on the initial displacements x_0 and y_0 , and the initial radial velocities \dot{x}_0 and \dot{y}_0 . The axial velocity at entry is important to the extent that it must be of low enough magnitude to ensure that the ion stays in the electric field long enough to separate the ions of adjacent mass numbers for a given resolution. An increase in resolution i.e. an increase in the U/V ratio has the effect of increasing sharply the amplitude of ion oscillation. Thus for given initial conditions an increase in resolution is accompanied by reduced ion transmission. So, in practice, a balance between resolution and transmission should be struck.

3. EFFECT OF INITIAL CONDITIONS ON ION TRANSMISSION

3.1 Maximum Amplitude of Ion Oscillation:

It was shown earlier that in a practical device, not only must a confined ion have a stable trajectory, but also the maximum amplitude of this trajectory must be smaller than the field radius. This necessitates computation of maximum amplitudes of ion motion as a function of the initial displacements x_0 and y_0 , initial radial velocities x'_0 and y'_0 and initial phase ωt_0 for (a, q) values chosen in the region of interest in the stability diagram. The equations of motion were numerically solved using appropriate initial conditions x_0, y_0, x'_0, y'_0 and ωt_0 to determine the maximum amplitudes of ion trajectories. Fourth order Runge-Kutta method was used for this purpose. Computations were made for various operating points along the mass scan lines corresponding to resolutions in the range 70-1000. The maximum amplitude of ions was determined over 160 cycles of ion motion.

3.2 Results of Computation:

The ratio of maximum amplitudes of ions to initial position $\frac{x_m}{x_0}$ and $\frac{y_m}{y_0}$ are plotted against 'q' values for resolutions 100, 200, 500 and 1000 in Fig.6. The 'a' values at which the computations are done are those corresponding to the given resolutions. The initial position of ions is $x_0=y_0=0.01$ inch (the amplitudes can, however, be arbitrarily scaled) and the radial velocity at entry is $x'_0 = y'_0 = 0.005$ inch/rad. The

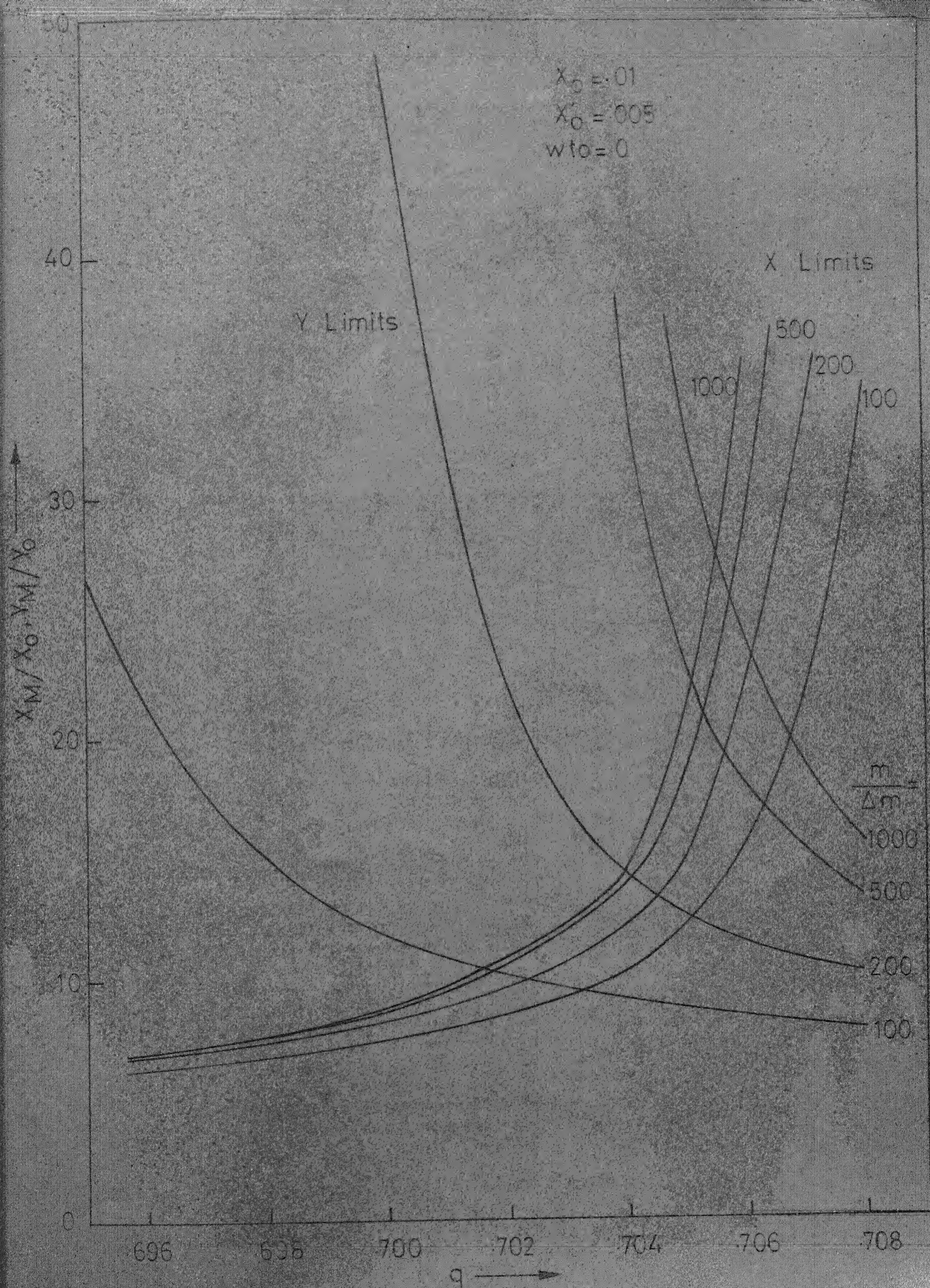


Fig. 6 -Maximum amplitudes at different resolutions

The initial phase ωt_0 is zero.

The effect of change in initial radial velocity of ions for a resolution of 200 is shown in Fig.7. The initial displacement of ions is 0.005 inch and the initial phase at entry is zero. The initial radial velocities are 0.005, 0.0075, 0.0025 inch/rad. respectively. Similar results for a resolution of 500 are shown in Fig.8.

Fig.9 shows the effect of change of initial position at a resolution of 70. The radial velocity of ions at entry is 0.01 and phase at entry is zero.

The effect of initial phase on the maximum amplitude of ion motion are shown in Fig.10, for operating points along different iso- β lines. The initial position of ion at entry is 0.01 inch and the radial velocity at entry is 0.005.

Using the above plots the limiting values of 'q' where x and y amplitude equals field radius is determined for given initial conditions. Within this range of 'q' all stable ions are transmitted resulting in 100% ion transmission. These ranges for 100% ion transmission for given initial conditions of ions are represented by contours in Fig.11. The field radius is taken to be 0.350 inch to arrive at these 100% ion transmission contours.

Maximum amplitudes of ion motion computed for parameters x_0 , x'_0 , ωt_0 and β given by Paul (2) agree within 1% to Paul's computations (2).

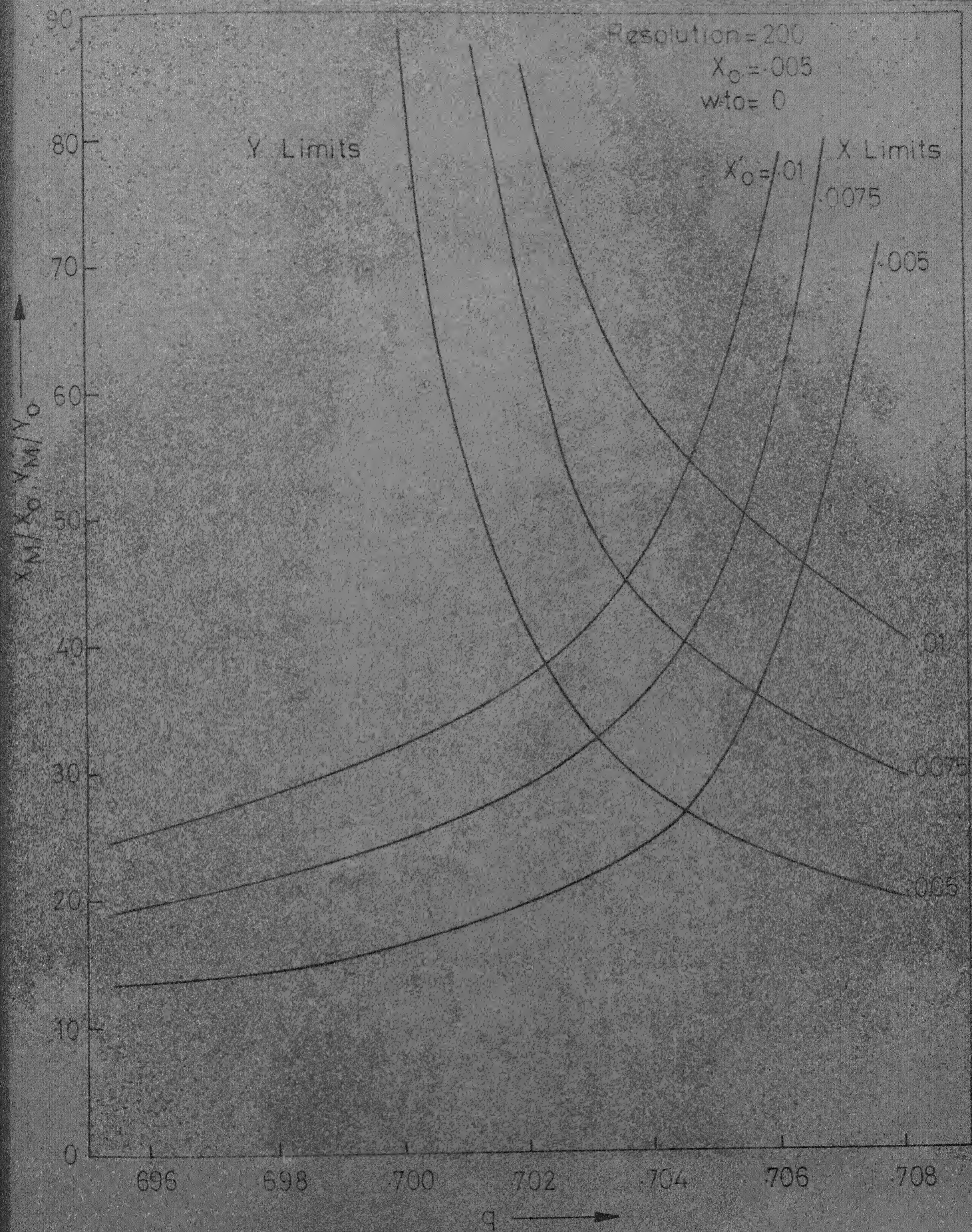


Fig. 7 - Effect of initial radial velocity at 200 resolution

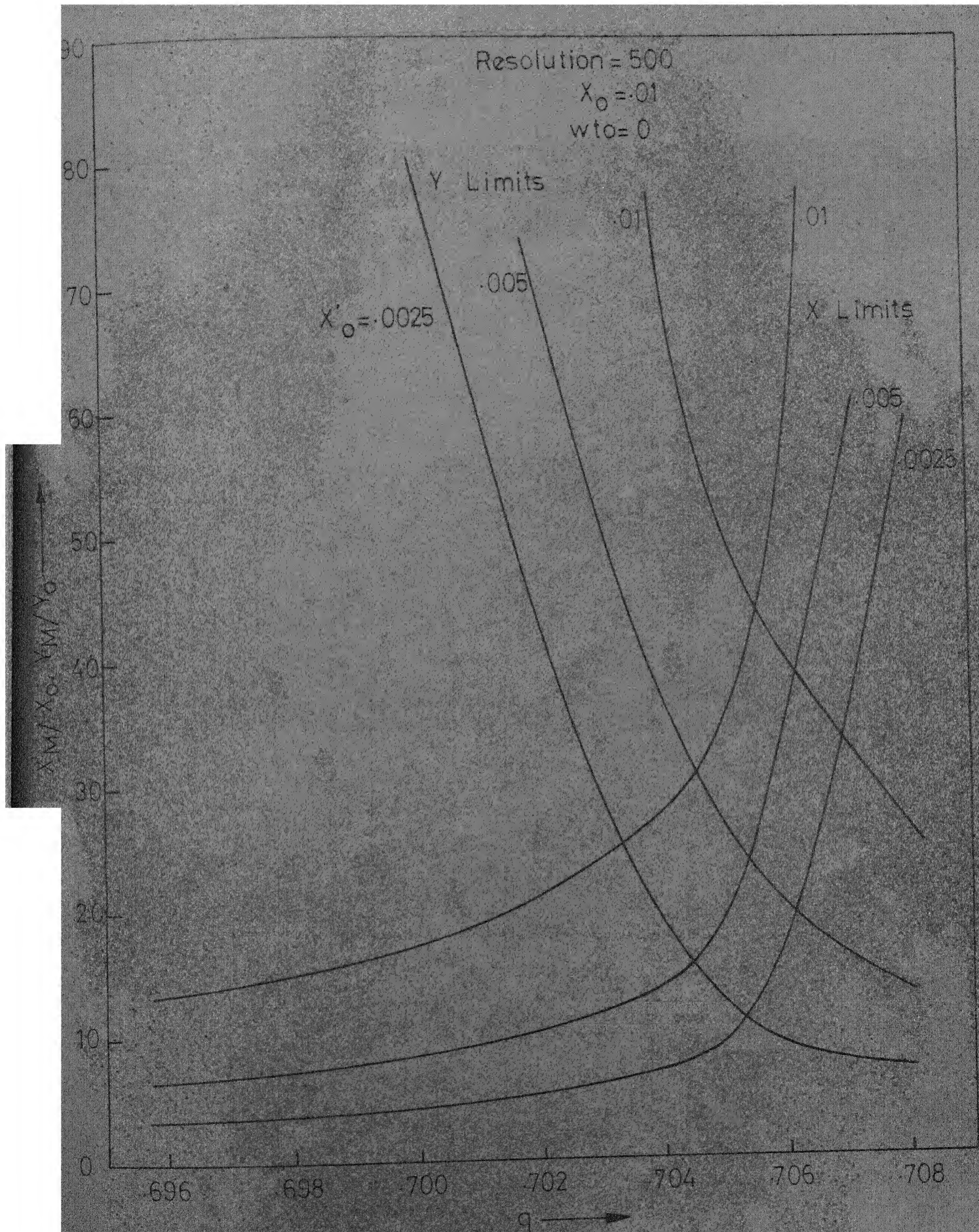


Fig. 8 - Effect of initial radial velocity at 500 resolution.

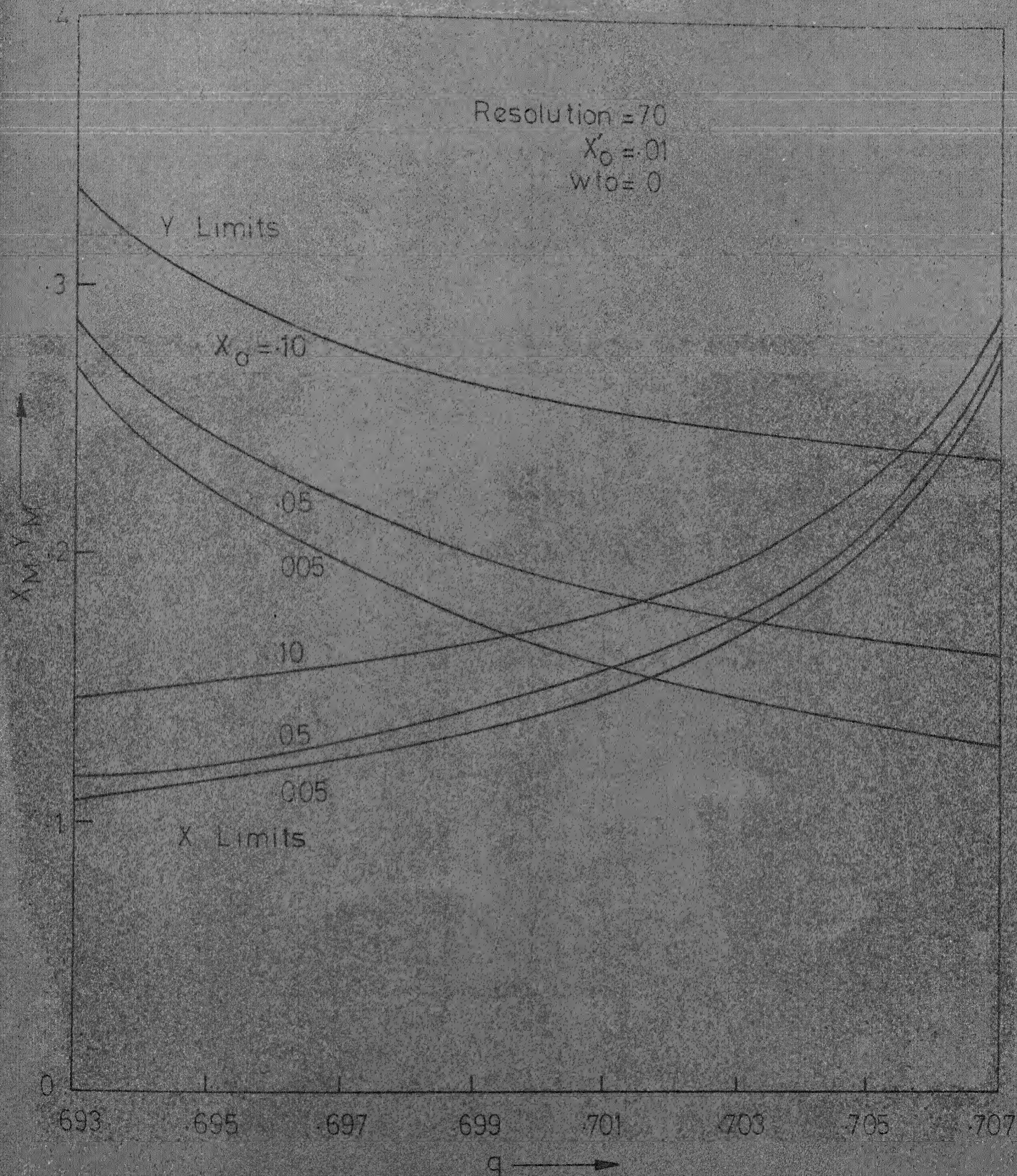


Fig. 9 - Effect of initial displacement at 70 resolution.

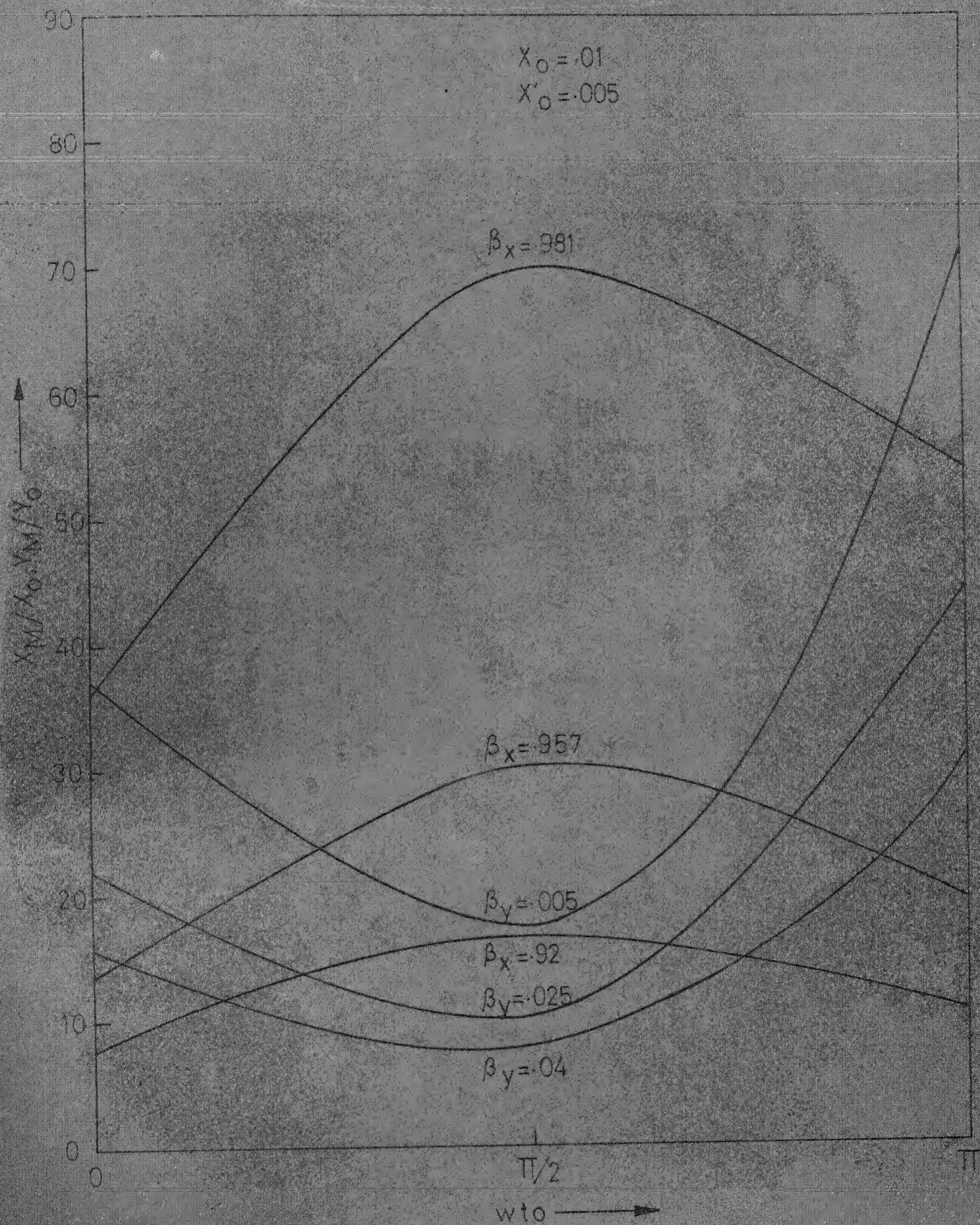


Fig 10-Effect of initial phase at different β values.

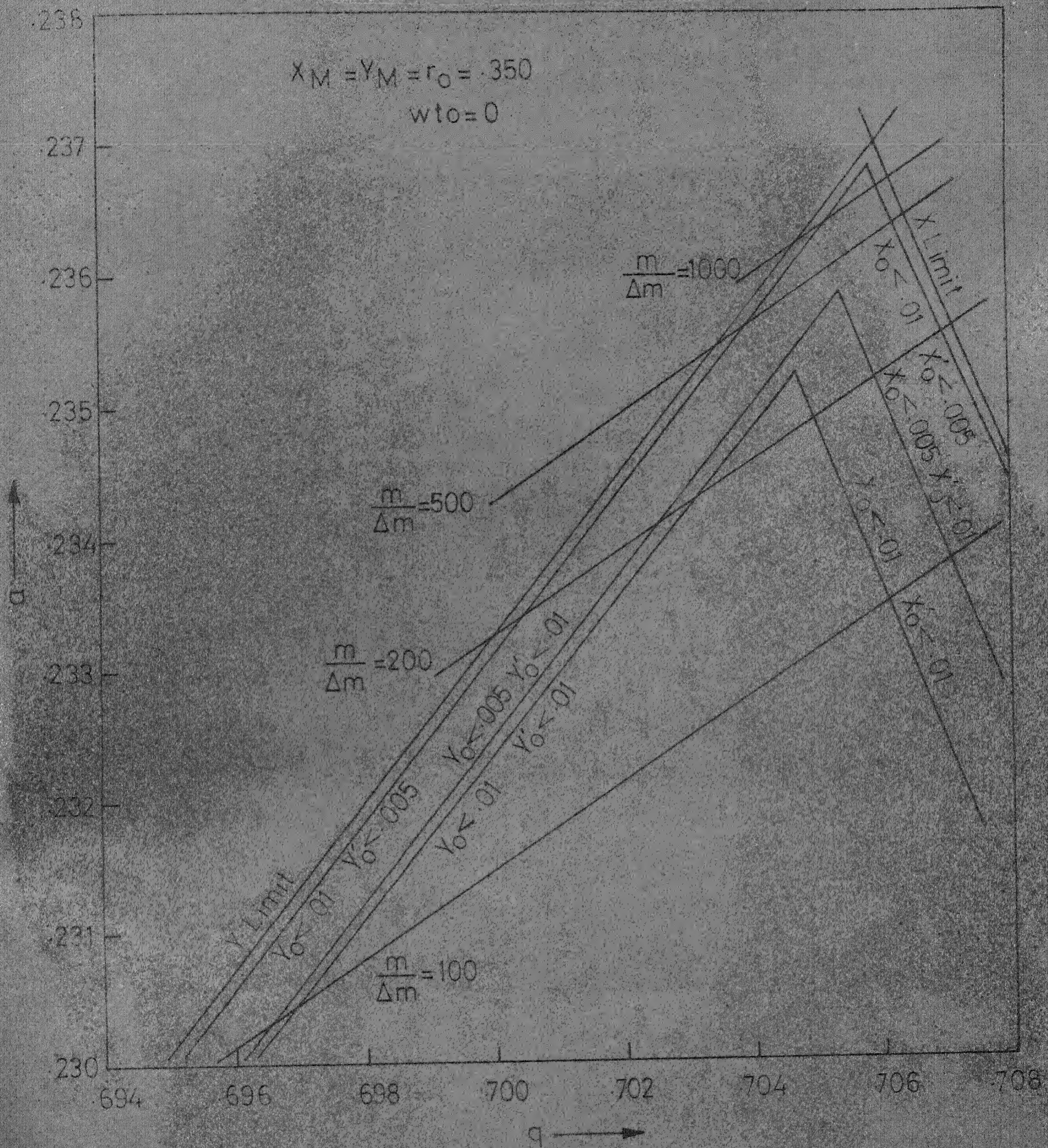


Fig 11 - 100% Ion transmission contours.

3.3 Conclusions from Present Computations:

Considering the effects of initial position of ions and radial velocity at entry independently (i.e. either of them is zero while the other is non-zero) Paul (2) arrived at limiting values for x_0 and \dot{x}_0 as

$$2y_0, 2x_0 \approx r_0 (\Delta M/M)^{1/2} \quad \dots \quad (11)$$

$$\dot{x}_M, \dot{y}_M < 0.16 r_0 \omega (\Delta M/M)^{1/2} \quad \dots \quad (12)$$

for 100% ion transmission. The present computations with both initial conditions non-zero simultaneously yields the bounds given in Fig.11 for 100% ion transmission which are higher than the bounds given by Eq.11. and Eq.12. This is presumably due to the fact that these equations do not account for interaction effects when both initial conditions are non-zero. Brubaker (3) has experimentally observed that off-axis entry of ions (i.e. non-zero initial displacement) with non-zero initial radial velocity results in higher ion transmission than ion entry at axis (i.e. zero initial displacement). This implies that interaction effects (i.e. simultaneous non-zero initial conditions) result in higher bounds for 100% ion transmission than individual effects (i.e., either of the initial conditions is zero). These computed values are used in determining the limits of initial conditions for 100% ion transmission at given resolution.

4. QUADRUPOLE MASS SPECTROMETER DESIGN

4.1. Mechanical Design:

The ion source is of electron impact type. A schematic diagram is shown in Fig. 12. The electrons are emitted by a 5 mil diameter heated Tungsten filament. An accelerating potential applied between the filament and the ionisation chamber takes the electrons into the ionisation chamber. The sample to be analysed, from a sampling device, enters the ionisation chamber via a passage in the repeller. Electron impact ionisation takes place within the ionisation chamber and the electrons resulting from ionisation are removed at the anode which is on the other side of the ionisation chamber opposite to the filament. The positive ions produced in the ionisation chamber are repelled away by the repeller and enter into the mass analyser section through an entrance aperture of 0.020 inch diameter.

The mass analyser consists of four cylindrical rods in place of hyperbolic rods. They are arranged such that $r_{\text{rod}}/r_0 = 1.16 (2)$. This configuration results in best approximation of the hyperbolic field using cylindrical rods.

The quadrupole rods are 6" long and 3/8" in diameter and are machined accurate to 0.001 inch. The end supporting pieces on which these rods are mounted are obtained by cutting a machined piece into two parts. The mounting holes are bored and the alignment channels are cut before it is separated into

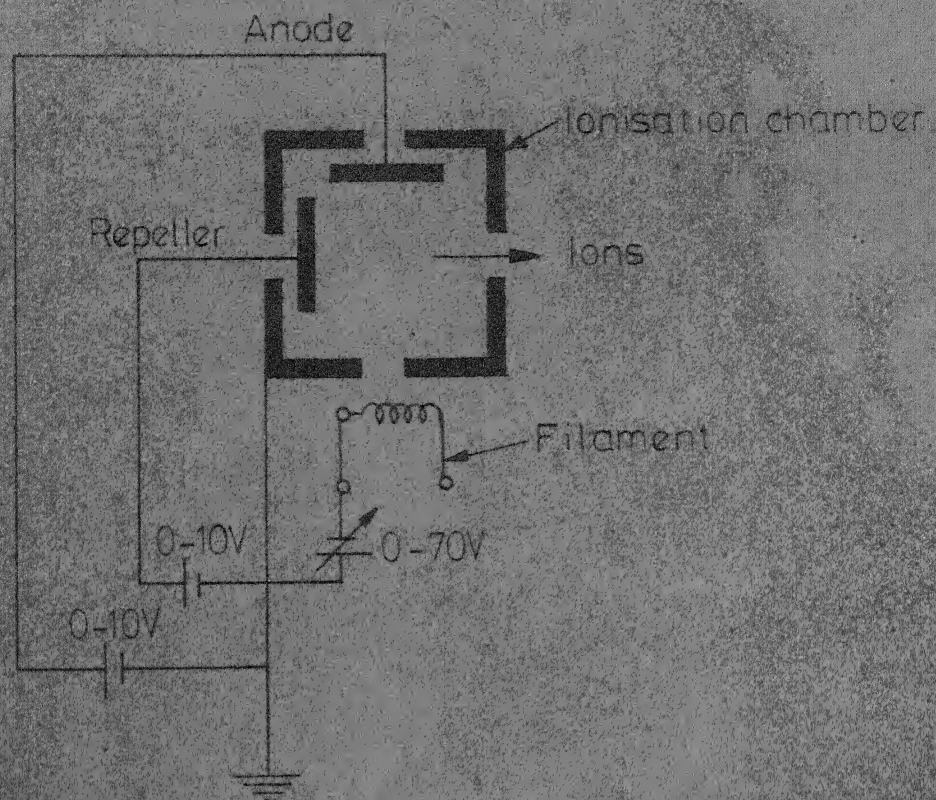


Fig.12-Schematic of Ion Source.

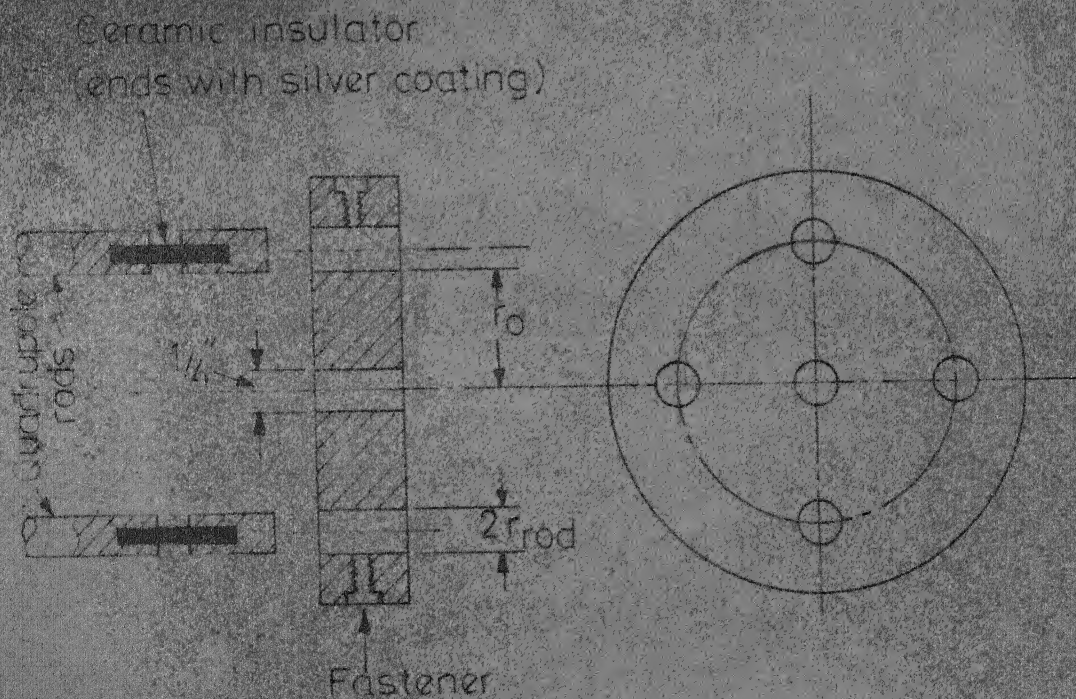


Fig.13-Schematic of Quadrupole Mounting.

two end pieces. The mounting of quadrupole rods is shown in Fig. 13. The alignment of the rods is accurate to 0.001 inch. The rods in the field region are insulated from the rod pieces at support by special ceramic insulators. These ceramic insulators are metal coated at their ends and are silver soldered to the quadrupole rods. By this way, the tolerance of quadrupole rod alignment is made independent of insulator non-uniformities.

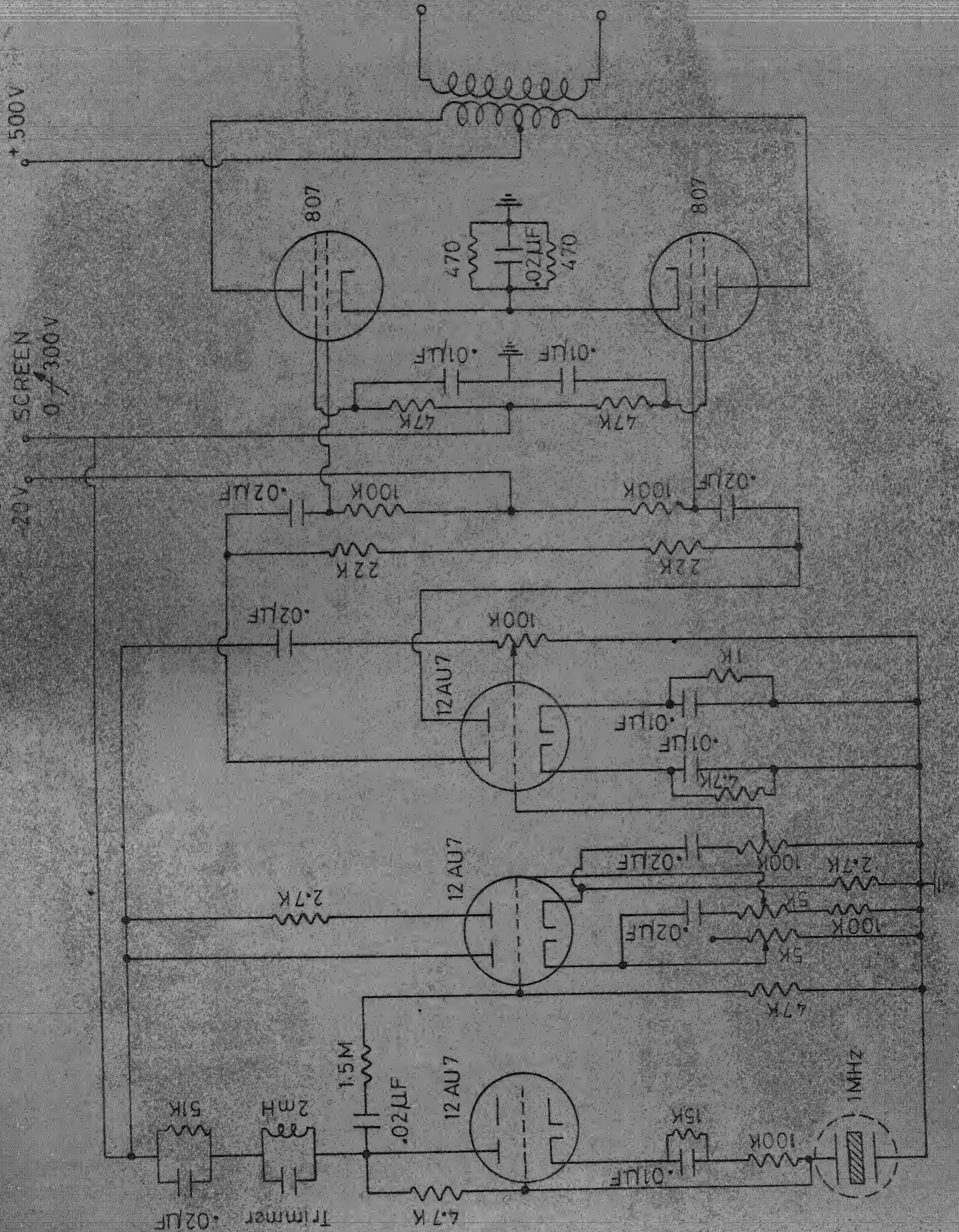
The ion collector used at the end of the quadrupole field is an RCA electron multiplier. It is a 14 stage Cu-Be dynode multiplier with a gain of 10^6 .

The whole assembly of ion source, analyser and electron multiplier ion collector is flange mounted. It is compact, light in weight and can be easily mounted on any system.

4.2. Electronic Design:

The electronic circuit to operate the quadrupole mass spectrometer is given in Fig. 14 and 15. The 1 MHz rf voltage is produced with a crystal oscillator and power amplifications of this rf voltage is accomplished in the tube circuit shown in Fig. 14. The dc voltage is obtained by rectifying a part of the rf voltage taken from an inductive voltage divider shown in Fig. 15. By this the constancy of the ratio between rf and dc voltages is ensured. The inductive voltage divider is grounded at centre thus symmetrising the field. Two potentiometers on either sides of this ground are used to vary

To ac/dc excitation matching network.



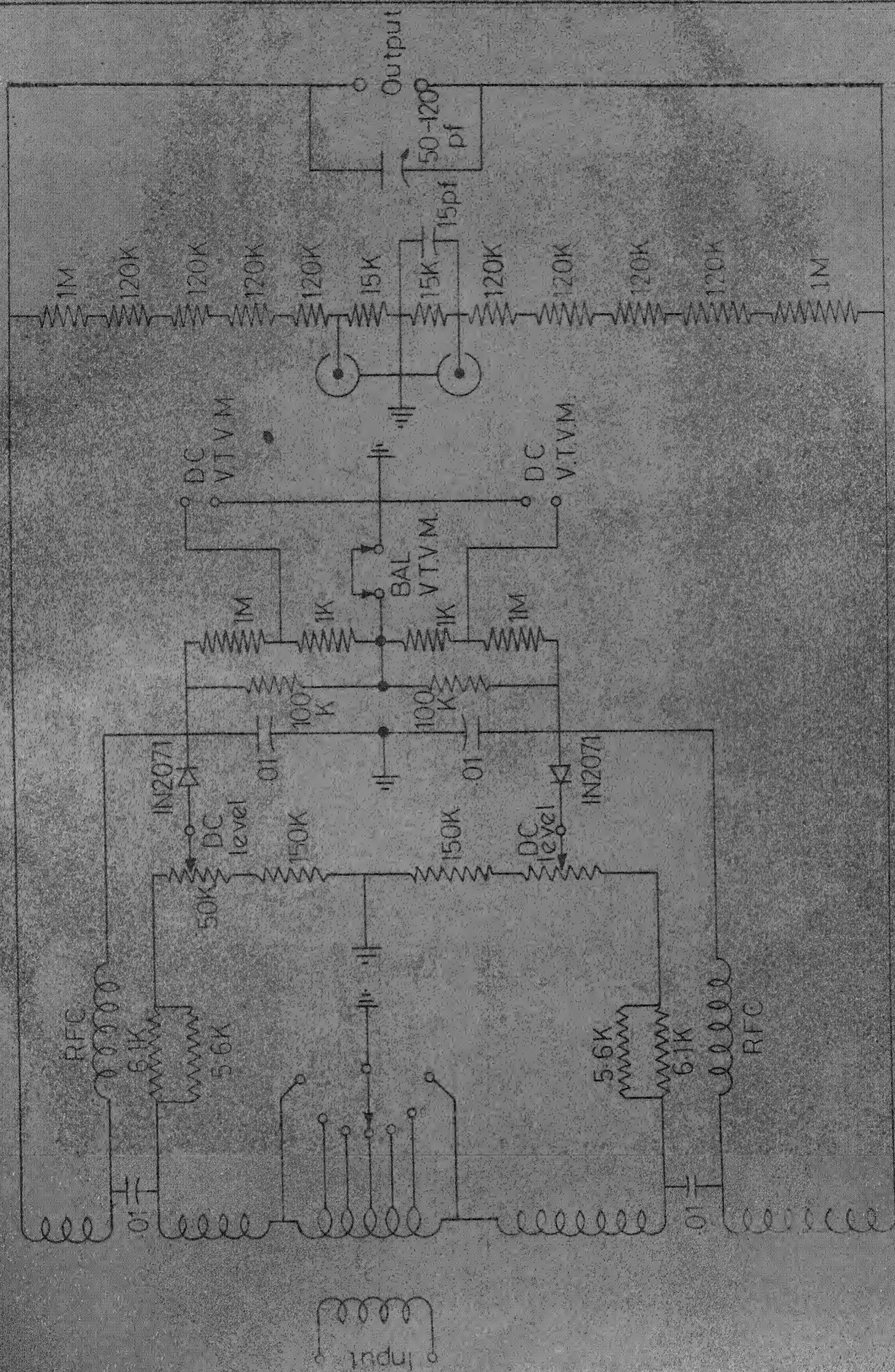


Fig 15-AC/DC excitation matching network.

+ 60V DC

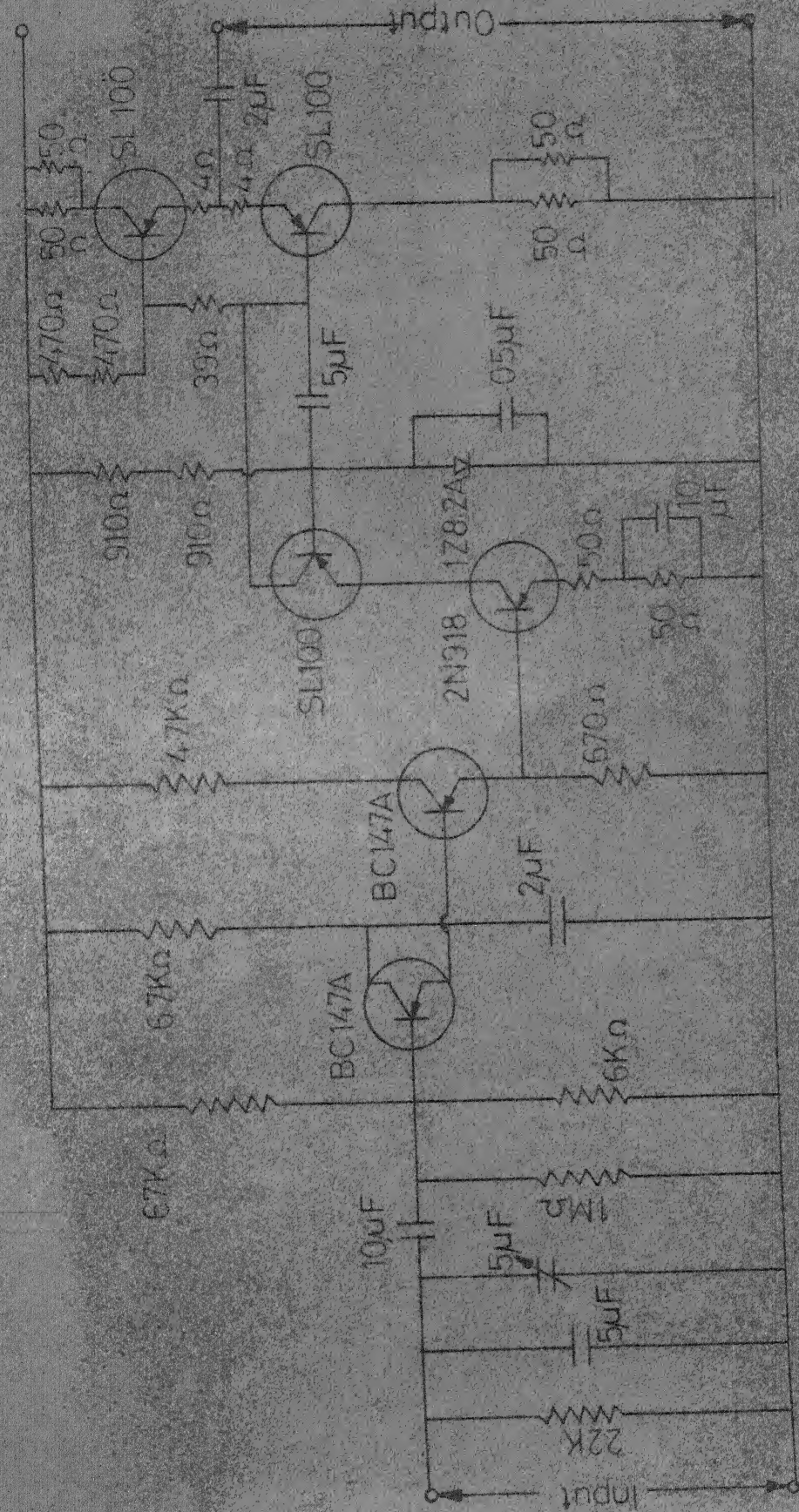
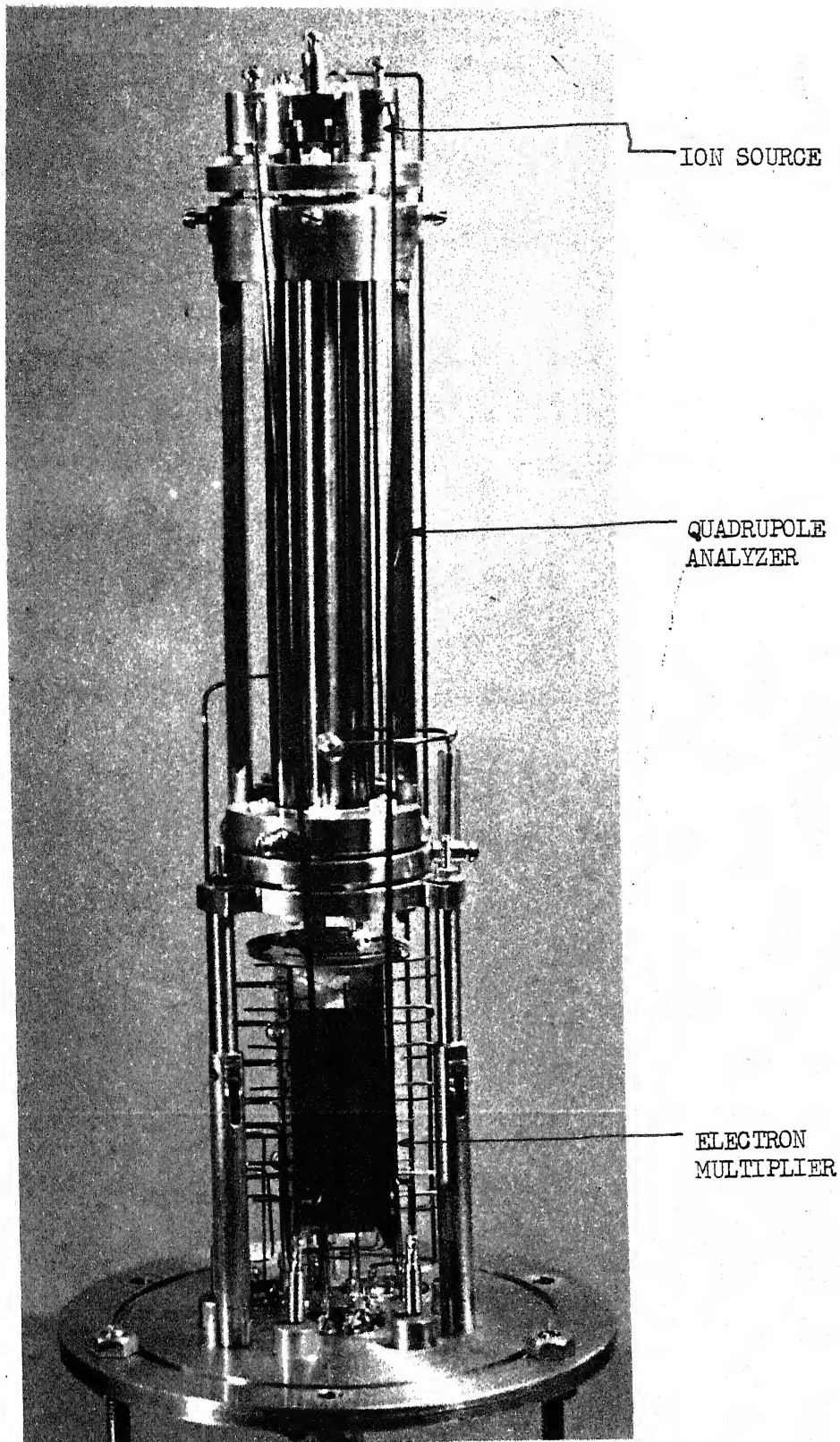


FIG. 16 - Transistorised P.A. amplifier.



INTERNAL PARTS OF THE QUADRUPOLE MASS SPECTROMETER
(approximately half the actual size)

the ratio U/V . The frequency is stable to 10^{-6} . But considerable difficulty is encountered in symmetrising the field. The mass scanning is accomplished by varying the screen voltage to the oscillator amplifier tube.

Fig. 16 gives an alternative transistorised circuit which was also used. This transistorised rf amplifier is used in conjunction with an oscillator (output voltage of 0-5 V) and the AC/DC matching network shown in Fig. 15. When this is used as the quadrupole power supply, the mass scanning is accomplished by varying the oscillator output voltage.

5. EXPERIMENTS, RESULTS AND CONCLUSIONS

The quadrupole mass spectrometer was tested with gas mixture containing N_2 , O_2 , Ar, NO, CO_2 . The operational pressure was about 10^{-5} mm Hg measured by an ionisation gauge. The predominant ions under these experimental conditions are N_2^+ , N^+ , Ar^+ , NO^+ , O_2^+ , O^+ , CO_2^+ . The unanalysed ion current is of the order of 10^{-11} ampere using 10^6 as the gain of the electron multiplier detector. The variation of the ion current is linear with pressure within experimental errors. Fig. 17 indicates some typical mass spectrums obtained with a sample of mixture of gases. The observed resolution of the mass spectrometer is significantly lower than the design value of 500.

For process control applications the ion current can be amplified and this amplified signal can be used as the controlling signal. The present flange mounted design of the mass spectrometer is ideal for its use as in situ controller.

Since the observed resolution of the spectrometer is significantly lower than the design value, further work is necessary to improve the resolution. As the present design of quadrupole mounting is close to the requirements, any increase in resolution can be achieved only with improvements in electronic design. Specifically, the voltage balance between either pair of the quadrupole rods should be improved and the constancy of the U/V ratio should be maintained. These

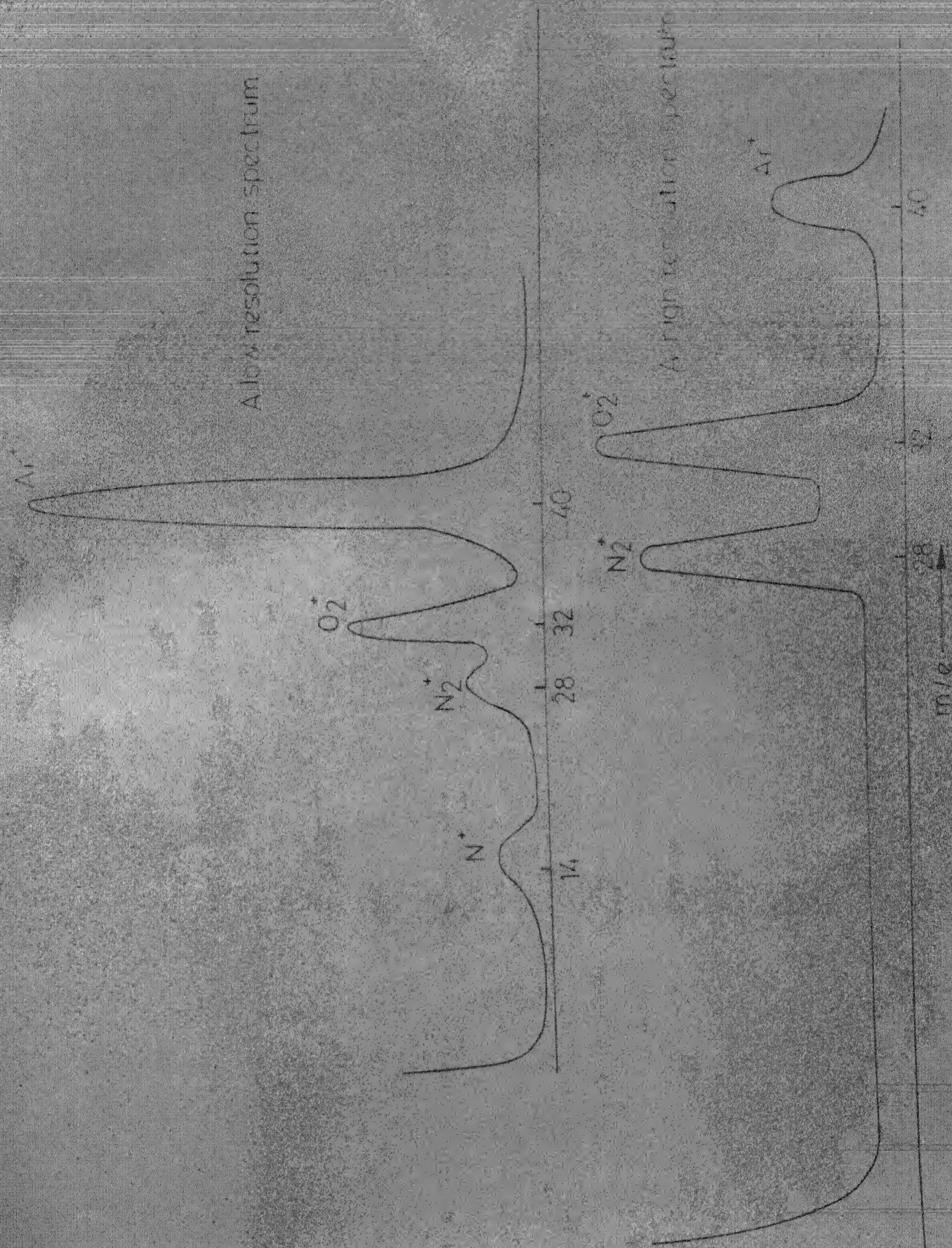


Fig 17 - Typical mass spectrum

two improvements should significantly increase the resolution. Also, developmental work for the fabrication of electron-multiplier particle detectors is to be taken up so that the RCA multiplier being used at present can be replaced by our own indigenous design.

REFERENCES

1. N.W. McLachlan in "Theory and Applications of Mathieu Functions", Oxford University Press, London and New York, (1951).
2. W. Paul, H.P. Reinhard and U. van Zahn, Z. Physik, 152, 143 (1958).
3. W.M. Brubaker, Colloq. Spectrosc. Intern., 9th, Lyon, France, June (1961).


```

C -----
C
C
C THIS PROGRAM COMPUTES THE MAXIMUM AMPLITUDES OF AN ION OSCILLATIONS
C IN THE -X- AND -Y- DIRECTIONS OF THE QUADRAPOLE FIELD FOR VARIOUS
C ENTRY CONDITIONS OF IONS SUCH AS POSITRON, RADIAL VELOCITY AND PHASE
C AT DIFFERENT MASS SPECTROMETER OPERATING POINTS.
C
C -----
C
CIBFTC MAIN
      DIMENSION AK(12),AL(12),FI(20),ZTEMP(500),FTEMP(500),XTEMP(500)
      DIMENSIONAB(4)
      INDEX=0
      I=1
      H=0.05

C
C
C AB(1)=0.23627 AND AB(2)=0.23667 CORRESPOND TO THE A(Q=0.706)
C VALUES FOR GIVEN MASS SPECTROMETER RESOLUTIONS
C
C
      AB(1)=0.23627
      AB(2)=0.23667
      DO107IJ=1,2
      AA=AB(IJ)
      PRINT111,AA
111  FORMAT(//2X,*AA=*F15.8//)
      RATIO=AA/0.706
      Q=0.696
105  Q=Q+0.003
      A=Q*RATIO
99   FI(I)=0.0
      K=0
      MAX=10

C
C
C ZETA=0.0 CORRESPONDS TO PHASE AT ENTRY
C XIN=0.005 CORRESPONDS TO POSITION AT ENTRY
C FINI=0.005 RADIAL VELOCITY AT ENTRY
C
C
C
59  ZETA=0.0
      XIN=0.005
      FINI=0.005
      XINI=XIN
      X=XIN
      FIN=FINI
      F=FIN
      PRINT 10,XIN,FIN,A,Q
10  FORMAT(4F16.8)
2   N=0
3   N=N+1
      ANGLE=2.0*ZETA+FI(1)
      PI=4.0*ATAN(1.0)

```

```

20 TEST=ANGLE-2.0*PI
   IF(TEST)17,17,19
19 ANGLE=TEST
   GO TO 20
17 PIHLF=ANGLE-PI/2.0
   IF(PIHLF)21,21,22
21 Y=COS(ANGLE)
   GO TO 27
22 PIONE=ANGLE-PI
   IF(PIONE)23,23,24
23 B=PI-ANGLE
   Y=-COS(B)
   GO TO 27
24 PITHR=ANGLE-(3.0*PI)/2.0
   IF(PITHR)25,25,26
25 Z=ANGLE-PI
   Y=-COS(Z)
   GO TO 27
26 Z=2.0*PI-ANGLE
   Y=COS(Z)
27 G=-(A+2.0*Q*Y)*X
   IF(INDEX-1)100,101,101
101 G=-G
100 AK(N)=H*F
   AL(N)=H*G
   X=XIN
   F=FIN
   IF(N-3)4,5,5
4 ZETA=ZETA+H/2.0
   X=X+AK(N)/2.0
   F=F+AL(N)/2.0
   IF(N-2)3,6,6
6 ZETA=ZETA-H/2.0
   GO TO 3
5 IF(N-4)7,8,8
7 ZETA=ZETA+H/2.0
   X=X+AK(N)
   F=F+AL(N)
   GO TO 3
8 AKSUM=(AK(1)+2.0*AK(2)+2.0*AK(3)+AK(4))/6.0
9 ALSUM=(AL(1)+2.0*AL(2)+2.0*AL(3)+AL(4))/6.0
   X=X+AKSUM
   F=F+ALSUM
   IF(XIN)37,38,38
37 IF(X)41,64,64
38 IF(X)64,41,41
41 IF(MAX)46,45,45
45 IF(X-XIN)48,48,64
46 IF(X-XIN)64,47,47
48 MAX=-10
   GO TO 51
47 MAX=10
51 K=K+1
   XTEMP(K)=XIN
   ZTEMP(K)=ZETA-H
   FTEMP(K)=FIN

```

```
64 XIN=X
   FIN=F
   X=XIN
   F=FIN
   IF(ZETA-80.0)2,11,1'
```

C
C
C
C
C
C

ZTEMP IS THE PHASE OF OSCILLATION WHEN THE MAXIMUM AMPITUDE IS XTEMP
FTEMP IS THE RADIAL VELOCITY WHEN THE MAXIMUM AMPITUDE IS XTEMP

```
11 PRINT82,(ZTEMP(L),FTEMP(L),XTEMP(L),L=1,K )
82 FORMAT(9E12.5)
   DO49KM=1,500
   ZTEMP(KM)=0.0
   FTEMP(KM)=0.0
49 XTEMP(KM)=0.0
   IF(INDEX-1)102,79,79
102 INDEX=INDEX+1
   GO TO 99
79 INDEX=0.0
   IF(Q-0.708)105,107,107
107 CONTINUE
900 CONTINUE
901 FORMAT(2F15.5)
   STOP
   END
```

ENTRY